European Journal of Radiology Open 8 (2021) 100369

Contents lists available at ScienceDirect

European Journal of Radiology Open

journal homepage: www.elsevier.com/locate/ejro

Review

Spinal vascular lesions: anatomy, imaging techniques and treatment

Valerio Da Ros [a,1], Eliseo Picchi [a,1], Valentina Ferrazzoli [b], Tommaso Schirinzi [c], Federico Sabuzi [a], Piergiorgio Grillo [c], Massimo Muto [d,e], Francesco Garaci [b,f], Mario Muto [e,2], Francesca Di Giuliano [b,2]

[a] Diagnostic Imaging Unit, Department of Biomedicine and Prevention, University of Rome Tor Vergata, Viale Oxford 81, Rome, 00133, Italy
[b] Neuroradiology Unit, Department of Biomedicine and Prevention, University of Rome Tor Vergata, Viale Oxford 81, Rome, 00133, Italy
[c] Neurology Unit, Department of Systems Medicine, University of Rome Tor Vergata, Viale Oxford 81, Rome, 00133, Italy
[d] Department of Neurosciences and Reproductive and Odontostomatological Sciences, University of Naples Federico II, Naples, 80100, Italy
[e] Department of Neuroradiology, A.O.R.N. Cardarelli, Naples, 80100, Italy
[f] San Raffaele Cassino, Via Gaetano di Biasio 1, Cassino, 03043, Italy

HIGHLIGHTS

- Vascular myelopathies include different aetiology and mechanism of damage.
- The level of the lesion and the localization within the SC correlates with the clinical symptoms.
- CT, MRI and angiography are essential for diagnosis and treatment playing a complementary role.
- MRI is the gold standard for the evaluation of spinal cord lesions.
- Spinal angiography is the gold standard for evaluation of spinal cord vasculature and vascular malformations.

ARTICLE INFO

Keywords:
Vascular spinal cord lesions
Vascular myelopathies
Spinal cord anatomy
Neuroimaging
MRI
Spinal angiography

ABSTRACT

Background: Vascular lesions of the spinal cord are rare but potentially devastating conditions whose accurate recognition critically determines the clinical outcome. Several conditions lead to myelopathy due to either arterial ischemia, venous congestion or bleeding within the cord. The clinical presentation varies, according with the different aetiology and mechanism of damage.

Purpose: The aim is to provide a comprehensive review on the radiological features of the most common vascular myelopathies, passing through the knowledge of the vascular spinal anatomy and the clinical aspects of the different aetiologies, which is crucial to promptly address the diagnosis and the radiological assessment.

1. Introduction

Vascular diseases of the spinal cord (vascular myelopathies) are uncommon but critical conditions, often presenting with sudden symptoms onset, resulting in disability and impacting on quality of life; a proper radiological examination is essential for correct diagnosis and treatment.

Vascular myelopathies refer to distinct clinical and radiological findings due to any abnormalities of the physiological spinal vascularity, depending on either impaired arterial blood supply or venous drainage, leading to spinal cord injury; haemorrhage in the spinal cord, known as hematomyelia, may also occur as consequence of underlying vascular lesions.

Clinical presentation of vascular myelopathies is variable, as the level of the lesion and the localization within the spinal cord correlate with different symptoms and signs. Although the differential diagnosis can be narrowed down to a certain extent on the basis of clinical presentation, a considerable clinical overlap with other aetiologies of myelopathy still exists; computed tomography (CT) and magnetic resonance imaging (MRI) plays a key role in characterization of the disease and provide useful clues for accurate diagnosis.

This article is aimed at reviewing radiological findings in the most

E-mail address: valentinaferrazzoli@hotmail.it (V. Ferrazzoli).
[1] These authors contributed equally to this work.
[2] These authors contributed equally to this work.

https://doi.org/10.1016/j.ejro.2021.100369
Received 30 April 2021; Received in revised form 23 June 2021; Accepted 4 July 2021

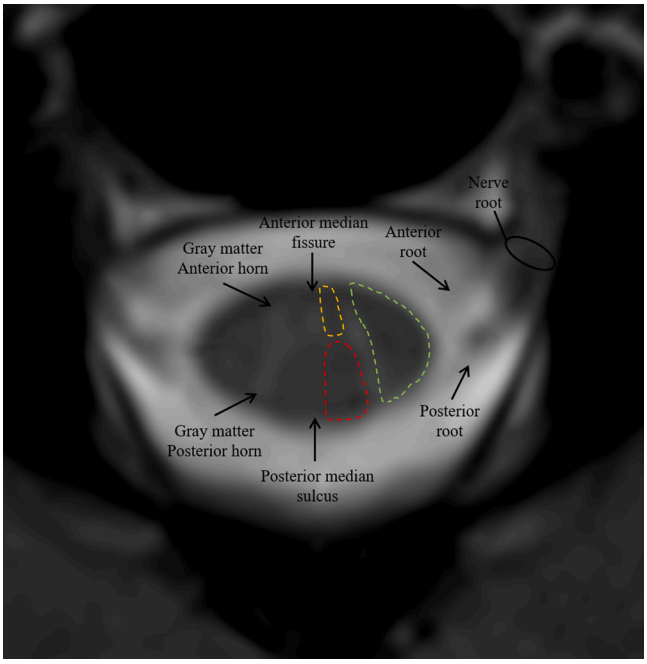

Fig. 1. Cross sectional MRI anatomy of the spinal cord in cervical segment. The grey matter appears hyperintense on T2 sequences and its H-shaped borders the three white matter columns: the anterior column (yellow dotted line), the lateral column (green dotted line) and the dorsal column (red dotted line) (For interpretation of the references to colour in this figure legend, the reader is referred to the web version of this article).

common spinal vascular lesions, focusing on imaging techniques including computed tomography, magnetic resonance and spinal angiography.

2. Spinal cord anatomy

The spinal cord is allocated in the vertebral canal and it is surrounded by three different layers: the dura mater, arachnoid, and pia mater. The *pia mater* is the innermost meninx with high dense small blood vessels penetrating the outer surface of the spinal cord; the denticulate ligaments, arising from the pia mater and attaching to the inner dura mater, suspend the spinal cord in the vertebral canal. Between the pia mater and the arachnoid there is the subarachnoid space, a real space filled with the cerebrospinal fluid (CSF). Arachnoid is closely adherent to the dura mater creating a virtual space known as subdural space. Outward the *dura mater* there is the epidural space, a fat space which contains spinal roots, small arteries, the vertebral venous plexus and the lymphatics vessels.

The thickness of the spinal cord is variable, with two enlargements respectively at cervical and lumbar level. The lower segment of the spinal cord is termed *conus medullaris*, which terminates between T12 and L1 in adults and it is anchored to the first coccygeal vertebra through a connective filament continuous with the pia mater called *filum terminale*.

The spinal cord has two cleft named anterior median fissure and posterior median sulcus. The anterior and the posterior nerve roots arise ventro-laterally and dorsal-laterally respectively and they join together giving rise to the 31 pairs of spinal nerves, each pair innervating a dermatome: 8 cervical, 12 thoracic, 5 lumbar, 5 sacral and 1 coccygeal. Below the apex of the conus medullaris the set of nerve roots is commonly known as *cauda equina*.

Referring to the macroscopic cross-section anatomy, the neuronal cells form the grey matter, the innermost part of the spinal cord with the well-known H- or butterfly-shape; it is composed by paired anterior and posterior horns joined by the gray commissure. At the thoracic level only, there are paired lateral horns between the anterior and posterior horns. The anterior horns contain motor neurons, the posterior horns are formed by neurons that receive somatosensory information from the body; the lateral horns contain neurons that innervate visceral and

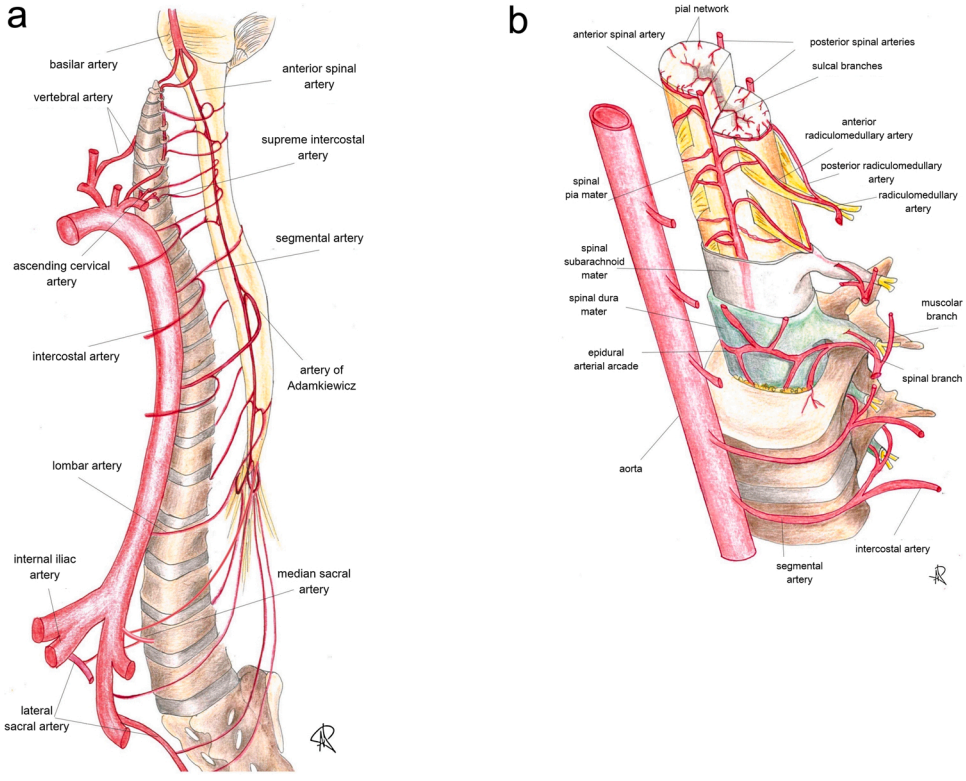

Fig. 2. (a and b). Sectional representation of the arterial blood supply and feeling vessels to spinal cord (see the text for further details), whose catheterization is mandatory during spinal angiography. Along the cranio-caudal direction, the angiographic study should include and demonstrate: vertebral arteries, ascending cervical arteries, deep cervical arteries (not shown), supreme intercostal arteries, intercostal arteries, lumbar arteries, median and lateral sacral arteries.
Identification of the artery of Adamkiewicz is essential, because spinal vascular malformations might themselves originate from this major feeder of the anterior spinal artery.

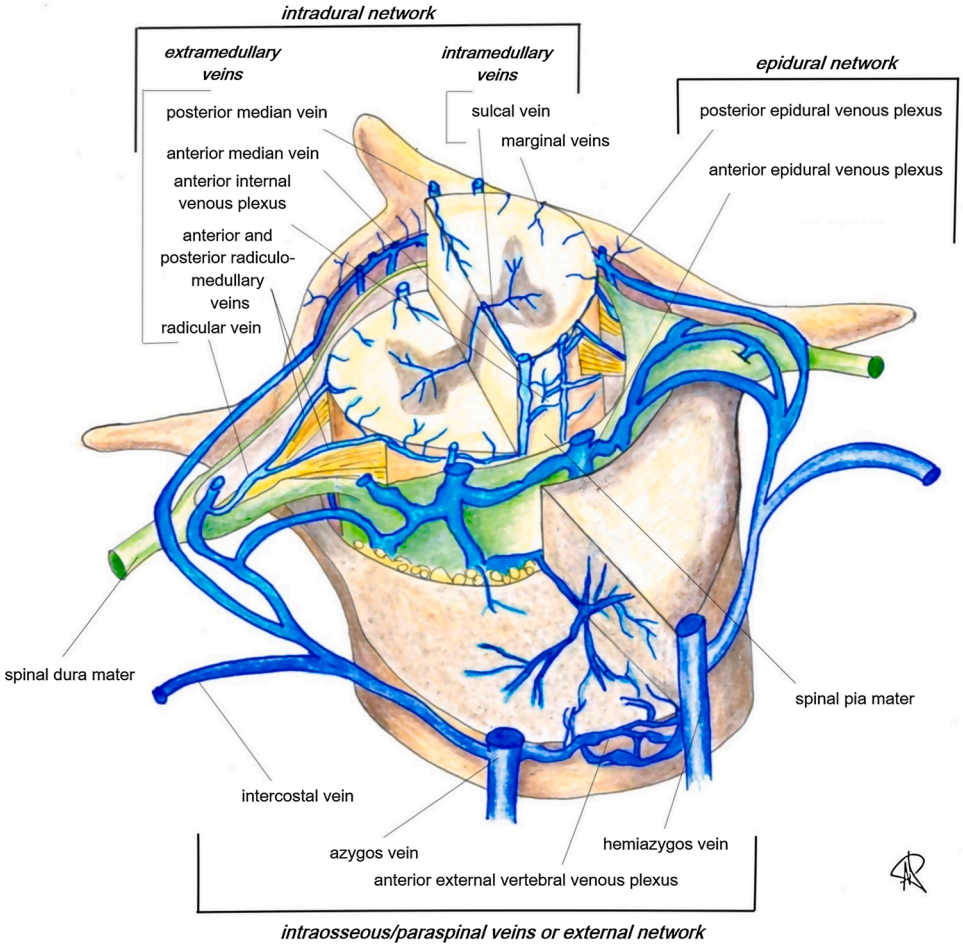

Fig. 3. Sectional representation of the spinal cord venous system (see the text for further details).

pelvic organs (Fig. 1).

The white matter surrounds the gray matter and it is composed of axons; the spinal white matter is organized in three main columns on each side: the dorsal column (between the posterior median sulcus and the posterior horn), the lateral column (between the posterior and anterior horns) and the anterior column (between the anterior horn and anterior median fissure). The white commissure joins the column of the spinal cord along the midline.

The white matter tracts constitute two motor descending pathways and three sensory ascending pathways. The descending pathways, located laterally and anteriorly, are the pyramidal tracts, controlling skilled voluntary movements, and the extrapyramidal tracts, a complex system for involuntary movements control. The ascending pathways carry sensory information as regards pain, temperature, coarse or fine touch, vibration and proprioception, from the periphery to the cortex or the cerebellum; they are, from the dorsal to the anterior columns respectively, the dorsal column medial lemniscus system, the spinocerebellar tracts and the anterolateral system.

The knowledge of spinal cord blood supply is challenging, due to both its inner anatomical complexity and often confusing nomenclature. A thorough knowledge plays a key role for determining the appropriate diagnosis and planning safe therapeutic approach in case of vascular-related spinal abnormalities.

The development of spinal cord vascular network begins during the first weeks of pre-natal life, when 31 somites are formed after the segmentation of the paraxial mesoderm; each somite receives one pair of arteries arising from the dorsal aorta, termed segmental arteries.

Segmental arteries give multiple branches to supply the vertebral bodies, paraspinal muscles, dura, nerve roots and spinal cord [1].

Into adulthood, most of the thoracolumbar segmental arteries - from T3 to L4 – retain their paired disposition, arising from descending aorta [2] as posterior intercostal and lumbar arteries; in the upper thoracic tract – T1 and T2 - segmental arteries share a common origin, the supreme intercostal artery, whereas the cervical region is supplied by segmental branches of the vertebral arteries, ascending and deep cervical arteries.

Arterial supply to L5 and the sacrum depends on segmental branches of the internal iliac artery (mainly the iliolumbar and lateral sacral arteries) and the median sacral artery.

Apart from vertebral, muscular and cutaneous branches, segmental arteries give off a spinal trunk which enters the spinal canal at the intervertebral foramen and provides the retrocorporeal, prelaminar and radicular arteries. The latter supply the dura and anterior and posterior nerve roots at each level; if involved in the vascularisation of the spinal cord, radicular arteries are termed as radiculomedullary (RMA), further divided into anterior radiculomedullary and radiculopial (or posterior radiculomedullary) arteries, based on whether they supply the anterior or posterior spinal arteries [3] (Fig. 2).

Only few RMAs are functionally important in adults, as most of them degenerate during the development [4], with high interindividual variance in number and size [3].

Anterior and posterior RMAs take part in formation of the anterior spinal artery (ASA) and the paired posterior (or postero-lateral) spinal arteries (PSAs), longitudinal trunks which run all along the spinal cord.

The ASA stems from the V4 segment of vertebral arteries, just below the vertebro-basilar junction, and runs in the anterior median sulcus; due to its long course, the ASA is fed at various levels by anterior RMAs, richly anastomosed to each other [5].

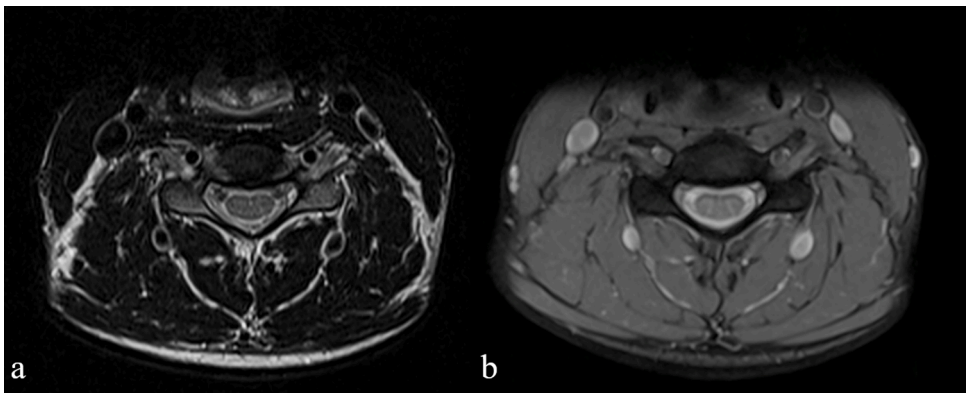

Fig. 4. T2 weighted images on axial plane in the same patient; a) T2-TSE sequence and b) T2-GRE sequence. To note the better identification of central grey matter in cervical spine in GRE than TSE sequence related to lower sensitivity of the pulsation artifact for the GRE sequence in the cervical spinal cord.

The most important anterior RMA is the artery of Adamkiewicz (AKA). Its origin is extremely variable, although in 89 % of cases it can be identified between T8 and L1; the origin from the left side is the most common [6]. In joining the ASA, the AKA forms a typical *"hairpin"* loop and gives off a large descending branch which goes down to the conus medullaris where it joins the posterior spinal arteries forming the periconal anastomotic circle, or "*basket*", which connects the anterior and posterior spinal circulations.

The two PSAs originate from the vertebral arteries or the posteroinferior cerebellar arteries (PICAs) and runs along the postero-lateral surfaces of the spinal cord. Similarly to the ASA, they are fed at various levels by the posterior RMAs (radiculopial arteries); after their origin PSAs become discontinuous and merged in a posterior pial plexus [1,3].

The pial plexus, also known as vasocorona, is formed by transverse and oblique branches from the ASA and PSAs and supplies the periphery of the spinal cord through perforating arteries; the sulcocommissural arteries instead, from ASA, course in the anterior median fissure. These intrinsic intramedullary arterial systems, respectively centripetal and centrifugal, are responsible for the arterial supply of the spinal cord tissue [7].

Likewise, as the arterial system, the spinal cord venous system is formed by intrinsic and extrinsic channels. The intrinsic system consists of sulcal and radial veins, which drain respectively in the longitudinal anteromedian and posterior spinal veins (posteromedial and posterolateral), connected by a coronary plexus. The longitudinal anterior and posterior veins drain via the radiculomedullary veins (RMVs) in the internal (epidural) anterior and posterior vertebral venous plexus; as a RMV crosses the dura, an antireflux valve-like structure is formed, preventing blood reflux from the epidural veins and demarcating the intradural and extradural venous compartments (Fig. 3).

The internal vertebral venous plexus runs along the spine within the vertebral canal and passes superiorly through the foramen magnum to join the intracranial venous system, forming a valveless, bi-directional plexiform venous network (the cerebrospinal venous system). Blood from this plexus drains into intervertebral and eventually segmental veins, which join the superior vena cava via the azygos systems [1,4,8].

3. Imaging techniques

3.1. Magnetic resonance imaging of the spinal lesions

MR is the gold standard for the evaluation of spinal cord lesions. The identification of the level of the lesion and the localization within the SC correlates with the clinical symptoms and signs. The differentiation between lesions that involve more or less than three segments is important to narrow the differential; in the former the differentials for longitudinally extensive transverse myelitis (LETM) are considered. Moreover, the identification of some patterns of T2 signal abnormality and/or enhancement may help in the diagnosis.

Crucial for a good-quality spinal examination is the use of high field strength magnetic resonance scanners ($\geq$ 1.5 T) that, thanks to higher spatial resolution and signal-to-noise ratio (SNR), allow greater radiologist's confidence in image analysis.

The standard spine MR protocol has to include at least two-dimensional (2D) Fast Spin Echo (FSE) T1- and T2-weighted sequences on the sagittal plane, using small field of view and slice thickness up to 3 mm, and T2-weighted sequences on axial plane centered at the clinical metameric level. The T2-weighted sequence with Short-Tau Inversion Recovery (STIR) technique is useful for spinal cord evaluation as it enhances spinal cord abnormalities thanks to its short Time Inversion value, which null the signal from fat; moreover, the T2-STIR signal is more homogenous with respect to the spectral fat saturated sequences as reported by Shah and Hanrahan [9]. However, T2w-STIR sequences showed lower signal-to-noise ratio (SNR), lower inter-reader agreement and greater sensitivity to motion and flow artifacts than SE or TSE sequences [10–13].

For the axial imaging, parallel to the intervertebral disk, 2D FSE or gradient recalled echo (GRE) sequences may be used. FSE sequences are commonly used to image the thoracic spinal cord and the spinal nerve roots in the lumbar tract, while GRE sequences showed greater sensitivity for the cervical spinal cord as GRE sequences, on axial plan, they have significantly lower flux artifacts for the cervical spine [14] (Fig. 4). Moreover, GRE sequences are useful for the study of the cervical spinal cord thanks to superior gray-white matter differentiation, greater sensitivity for the identification of spinal lesions and lower sensitivity to pulsation artifact, providing better depiction of the normal H – shaped central grey matter [15]; moreover, GRE sequences allow to depict intraspinal hemorrhage and the spinal cord cavernous malformations [16]. On the other hand, GRE sequences are affected by higher false-positive rate in spinal cord, also in healthy subjects, and may overestimate narrowing of the spinal canal due to degenerative process; moreover, the motion artifacts severely degrade GRE sequences with blurring of the central gray matter increasing the risk of false-positive.

In our experience, the use of three-dimensional (3D) gradient-echo T2-weighted sequence is not recommended due to its intrinsic lower soft-tissue contrast compared to 2D-T2-TSE sequences. Surely the 3D gradient-echo T2-weighted sequence is able to easily demonstrate intramedullary lesions with high water content, however the capacity in identifying hyperintense spinal lesions related to ischemia, edematous contusion and inflammatory-related alterations is lower [17].

Optional MRI sequences include Diffusion Weighted Imaging (DWI) with maximum b-value at 800 s/mm^2, which improves the diagnostic accuracy for the spinal ischemic insults and the depiction of infective collections, and the T1-w fat-suppressed images whose utility depends on the specific clinical questions. DWI has a very short acquisition time

Table 1
MR protocol for imaging spinal cord vascular lesions. SC: spinal cord; FOV: Field Of View; WI: weighted imaging; STIR: Short Inversion Tau Recovery, GRE: Gradient Recalled Echo; FSE: Fast Spin Echo; DWI: Diffusion Weighted Imaging.

MRI SEQUENCES	FOV (mm^2)	Slice thickness (mm)	Acquisition matrix	TR/TE (ms)	b-value (s/mm^2)
Sagittal T2-WI TSE	180 × 372 × 56	3	200 × 385	2500–4500/90	–
Sagittal T1- WI TSE pre and post contrast-medium	180 × 368 × 57	3	180 × 368	400–650/10	–
Sagittal STIR	180 × 372 × 65	3	188 × 320	2500–5500/65	–
Axial T2-WI GRE (cervical SC)	200 × 153 × 49	3	252 × 192	700–800/8	–
Axial T2-WI TSE (dorsal SC)	160 × 160 × 132	3	200 × 190	3000–5000/100	–
DWI- (sagittal plane)	220 × 198 × 33	3	80 × 70	3500/15	0–800

but is very sensitive to local magnetic field inhomogeneities and its daily clinical application is commonly reserved to ischemic changes.

The suggested MRI protocol for imaging spinal cord vascular lesions is summarized in Table 1:

Diffusion Tensor Imaging (DTI) is an advanced MRI technique which allows to non-invasively map the diffusion process of molecules in biological tissues. Surely, the use of 1.5 T MR scanners allows better compromise between geometric artefacts and temporal resolution. Its clinical application should be limited to ischemia, surgical planning for spinal cord tumors and for the follow-up in degenerative cervical myelopathy [18–21].

The contrast enhanced MR of the spinal cord is mainly useful to evaluate the neoplastic and the inflammatory diseases; the use of Gadolinium based contrast agent with high relaxivity allows to obtain higher signal intensity on T1-weighted MR sequences.

However, the main limitation of MR is the longtime of examination which depends on patient's collaboration and number of sequences included in the protocol. To reduce the scan time, Dixon-type pulse sequences, based on the different rates of precession of water and fat molecules, may be used [22]. Dixon sequences allow to obtain four different T1 or T2 weighted images (In-phase, Opposed-phase, Water--only and Fat-only images) combining different echoes acquired at different Time of Echo with mathematical formulas.

Recently the use of the 3D phase-sensitive inversion recovery (PSIR) sequence at 3 T scanner reported an improvement in spinal cord lesions' detection in patients suffering from multiple sclerosis, with higher lesion contrast and higher inter-reader agreement [23]. However, 3D-PSIR for the spinal analysis has a long acquisition time (up to 4 min just for the cervical segment) making its routinely clinical application less feasible. However, PSIR sequences remain still available for research and are not registered for clinical use and application.

In the future, the optimization of the spinal synthetic MRI (SyMRI) is highly recommended. SyMRI is a technique based on a quantitative approach, that allows the quantification of absolute-tissue physical properties by the acquisition of a single sequence obtaining images with different weighted (T1, T2, STIR, PD, PSIR); this means a potentially significant reduction of the acquisition time with the aim, still under investigation, to not reduce the diagnostic accuracy [24,25].

In spinal vascular malformations (SVMs), digital subtraction angiography (DSA) is the gold standard for the diagnosis and characterization, however MR angiography with contrast injection can non-invasively provide preliminary information that can reduce angiography duration and, consequently, radiation exposure and contrast dose. In arteriovenous fistula, conventional MRI cannot exactly identify the level affected; MR angiography with contrast injection has a good spatial and temporal resolution and allows to identify the level and side of the fistula, the feeding artery and the draining perimedullary vein, the level of AKA [26].

Contrast enhanced-magnetic resonance angiography (CE-MRA) consists in a rapid 3D T1-w spoiled GRE pulse sequence with short repetition and echo time that guarantees good spatial resolution, high SNR and no flow-related artefacts [27]. Through time-resolved acquisitions, an imaged volume is acquired over subsequent time points after contrast medium injection and a dynamic study in the arterial, venous, late and delayed phase is obtained. This technique allows to display the contrast passage through small vessels and, according with the Toronto experience, CE-MRA at 1,5 T correctly identified the level of spinal dural arteriovenous fistulas (SDAVFs) in over 80 % of cases and of other SVMs in 60 % of cases [28].

More recently 4D time-resolved MRA has been implemented and sequences as time-resolved angiography with keyhole acquisition (TRAK) or time resolved angiography with stochastic trajectories (TWIST) have been introduced in neurovascular imaging. Compared with CE-MRA, they have a much higher temporal resolution, accelerating dynamic scans up to 60 times; moreover, at 3 T field strength, they guarantee a nearly isotropic spatial resolution of 1 to 1,5 mm [29].

The use of maximum intensity projection (MIP) and multiplanar recontructions (MPR) helps in SVMs evaluation, providing images which are anatomically similar to 3D-DSA.

3.2. *Computed tomography angiography (CTA)*

The spinal cord is poorly visualized in CT images, however, the use of iodinated contrast agent, thanks to CT rapid acquisition and large field of view, allows the depiction of vascular anatomy. CTA is mainly used for the identification of the Adamkiewicz artery in pre-surgical planning for aortic dissection or aneurysm, in some cases for spinal tumors [30]. CTA allows fast scan of the whole spinal cord and opacification of all vessels responsible of SVMs, as well as enables optimal vertebral location [31]; high spatial resolution is ensured by using multi-slice detector CTs [32]. The drawback is the radiation dose.

3.3. *Spinal Angiography: when and how to perform it. The State of the Art*

Spinal angiography (SA) is the radiological *gold standard* for detailed evaluation of spinal cord vasculature and SVMs. Suspicion of SVMs usually raises after clinical and MR assessment, as previously described; SA follows conventional spinal MR imaging, preferably supplemented by non-invasive vascular evaluation performed with CE-MRA or CTA.

It is worth noting that, despite good reliability of both techniques, they do not replace conventional DSA in SVMs as confirmative test.

Arterial access for SA is usually accomplished through transfemoral route, after manual or ultrasound-guided retrograde puncture of the common femoral artery and insertion of a 4 or 5 F short sheath; transradial access for diagnostic and therapeutic SAs has previously been reported [33,34], especially in the setting of intra-operative angiograms [35], but the need of long catheters for distal thoracic and lumbosacral catheterizations as well as longer procedural times may represent a limitation for this technique.

No definitive conclusion can be inferred from literature concerning the best mode of anaesthesiology during spinal angiography. SA may be performed under local anaesthesia and conscious sedation or under general anaesthesia; the latter may be required in paediatric patients or in those unable to keep the supine position and avoid movements, given the long procedural time in most cases. Moreover, general anaesthesia allows better image quality and accuracy due to patient immobilization

[36] and the possibility to induce apnoea, if necessary, by blocking mechanical ventilation after intubation, avoiding multiple injections from the same vessel and reducing time needed to perform SA.

Once the femoral short sheath is placed, alignment of vertebral bodies and spinous processes must be checked to have images perfectly centred and not rotated. A radio-opaque marker, placed along the vertebral column, may simplify the examination working as a landmark during the whole SA, to avoid omissions or multiple injections of the same vessel.

In the setting of SVMs, a complete angiographic study of the cerebrovascular axis should be considered, including injections from bilateral carotid arteries, subclavian arteries and their branches, thoracic and lumbar segmental arteries, internal iliac arteries and medial sacral artery [37].

In some circumstances, SA may be tailored and limited in extension, especially when an SVM has been previously detected by non-invasive technique (such as MR) [4], obtaining significant dose and contrast load reduction. However, caution should be used when performing limited SA, as arterial collateral supply to the suspected SVM could be missed, resulting in an incomplete and potentially harmful examination. In our experience, we found safe and feasible to perform a focused SA at the level of suspected SVM plus two or three levels above and below to evaluate collaterals, when the clinical suspect of an SVM is high and both MRA and CTA have been performed; identification of the arterial supply to the ASA through RMAs or the artery of Adamkiewicz, as well as the dorsal arterial supply to the spinal cord via the radiculopial network, is mandatory after SVM identification.

SA execution as well as the choice of diagnostic catheters depend on operator's preferences and individual anatomy. Most SA often require the use of multiple catheters: reverse curve catheters like *Cobra* or *Simmons* usually enable access to thoracic and lumbar segmental arteries directly arising from aorta, whereas catheterization of subclavian branches and carotid arteries may be easily performed with simple curve catheters like *Vertebral* ones, unless unfavourable aortic arch or epiaortic vessels configurations.

Segmental arteries should then be accessed systematically, ideally in a cranio-caudal or caudo-cranial fashion one side at time, gently rotating and moving the catheter upward or downward; the catheter's tip should always be checked for little deflections, suggestive of arterial ostia engagement [4].

Before contrast injection, one should carefully flush the catheter lumen to aspire air bubbles or thrombi and clear the dead space; contrast injection is then performed with appropriate volumes and injections rates. We prefer hand injections to adapt flows and volumes to the vessel lumen and resistance and to prevent iatrogenic dissections of the smallest branches. It is mandatory to perform technically adequate injections during SA, avoiding non-selective injections which may results in a low-quality angiogram or false negative examination due to the poor amount of contrast in the target vessel [38]; on the other side, two or more segmental arteries may be filled with a single injection resulting in an overlapped – and non-diagnostic – opacification.

After bidimensional DSA and identification of SVMs, or in case of doubt, SA is usually integrated with a three-dimensional imaging protocol, nowadays part of the standard of care of SVMs [39]. 3D rotational DSA or 3D Conebeam CT angiography, acquired by selective intra-arterial contrast injection and following 3D reconstruction with dedicated software, provide with a single selective injection further information regarding the anatomy of SVMs (feeding arteries, draining veins, nidus), as well as relationship with normal vessels and surrounding bony structure. 3D imaging is essential for the proper endovascular treatment of SVMs, the choice of the best working projection and therapeutic strategy [40].

However, angiography is the gold standard in order to obtain exhaustive classification of the SVMs that should be categorized considering the location, the arterial feeder, the venous drainage, the internal structure (glomus or compact AVMs, diffuse AVM or AV fistulas) and the hemodynamic features of the SVM (high-, moderate- and slow-flow). These characteristics are well demonstrated by SA. In accordance to the above-mentioned technical points the SVMs have been categorized by Anson and Spetzler [41] as follows in Table 2:

Table 2
Classification of spinal arteriovenous malformation (AVM).

Type	Radiological criteria
1	AV Fistula located between a dural branch of the spinal ramus of a radicular artery and an intradural medullary vein
2	Intramedullary glomus malformation with a compact nidus within the substance of the spinal cord
3	Juvenile or combined AVMs -extensive AVM often extending to the vertebra or paraspinal tissues
4	Intradural perimedullary arteriovenous fistula
4a	simple fistula fed by a single arterial branch
4b	intermediate sized fistula with multiple dilated arterial feeders
4c	large perimedullary fistula with multiple giant arterial feeders

Table 3
Update classification of the spinal arteriovenous malformation (AVM); AVF: arteriovenous fistula.

Type	Definition
1	Dural AVF
2	Intramedullary glomus-type AVM
3	Intramedullary juvenile AVM
4	Perimedullary AVM
4a	A simple extramedullary fistula fed by a single artery
4b	An intermediate-sized fistula with mono- or bipedicled feeding arteries and dilated drainage veins
4c	Giant fistulas with multipedicled arteries of large caliber and dilated large varix
5	Extradural-paraspinal AVM/AVF
5a	With medullary venous drainage
5b	Without medullary venous drainage

Table 4
The main neurological findings in the vascular spinal cord lesions.

Functional syndrome	Anatomical tracts	Disturbances
Anterior cord	Corticospinal, spinothalamic, sympathetic	Tetraparesis or paraparesis, bilateral loss of pain – thermic sensitivity below lesion, dysautonomia
Posterior cord	Dorsal columns	Bilateral loss of tactile sensitivity, proprioception, and vibration below lesion
Complete cord	Corticospinal, spinothalamic, sympathetic, dorsal columns	Tetraparesis or paraparesis; bilateral loss of pain – termic sensitivity below lesion; dysautonomia; Bilateral loss of tactile sensitivity, proprioception, and vibration below lesion
Hemicord or Brown-Séquard syndrome	Corticospinal, spinothalamic, sympathetic, dorsal columns	Ipsilateral hemiparesis; contralateral loss of pain – thermic sensitivity from two dermatomes below lesion; Ipsilateral loss of tactile sensitivity, proprioception, and vibration below lesion
Central cord	Corticospinal, spinothalamic	Upper extremity weakness >> Lower extremity weakness, Bilateral loss of pain – thermic sensitivity suspended (only at level of injury) or complete below the lesion, urinary dysfunction

In 2019 Islak and N Kocer [42] reported an update of the previous classification adding another type of SVM if the spinal cord as follows in Table 3:

Spinal angiography has to be carefully evaluated considering the crucial role in diagnostic and pre-operative planning; attention must be

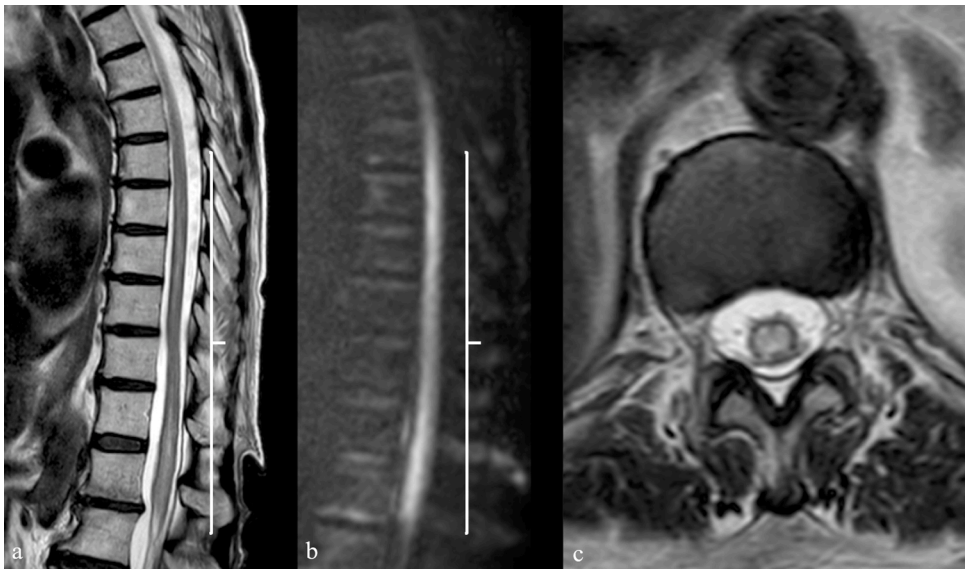

Fig. 5. Sagittal T2-TSE (a) and Diffusion Weighted (b) sequences in a 74 years old female patient with acute spinal ischemia. Axial T2-TSE sequence on axial plane (c) at level D12-L1. Diffusion weighted sequence clearly shows the restricted diffusion of the dorsal spinal cord (white brackets in b) corresponding to the hyperintense signal in the sagittal T2 sequence (white brackets in a); T2 sequences depicted a moderately swollen appearance of the medullary conus and the full involvement (grey and white matter) of the spinal cord.

paid to avoid technical or procedural error and the nonrecognition of documented lesions which are reported as the most common error [38]. A double reading of the image and a good training should avoid the non-recognition of the lesion.

4. Vascular lesions of the spinal cord

Vascular myelopathies may result from ischemia, venous congestion, arteriovenous malformation and haemorrhage.

Vascular diseases of the spinal cord are a group of rare but potentially devastating conditions, whose early and accurate recognition is fundamental for patients' outcome. Basically, we could acknowledge the spinal cord ischemia and the venous congestive myelopathy, the spinal cord haemorrhage and spinal vascular malformations. Traditionally spinal cord lesions cause different clinical syndromes depending on the involved tracts as reported in Table 4. However, every single clinical entity may present with peculiar features; as well, the therapeutic approach may differ. Attention must be paid to inflammatory conditions which might present with acute onset and the same neurological symptoms and signs [43,44].

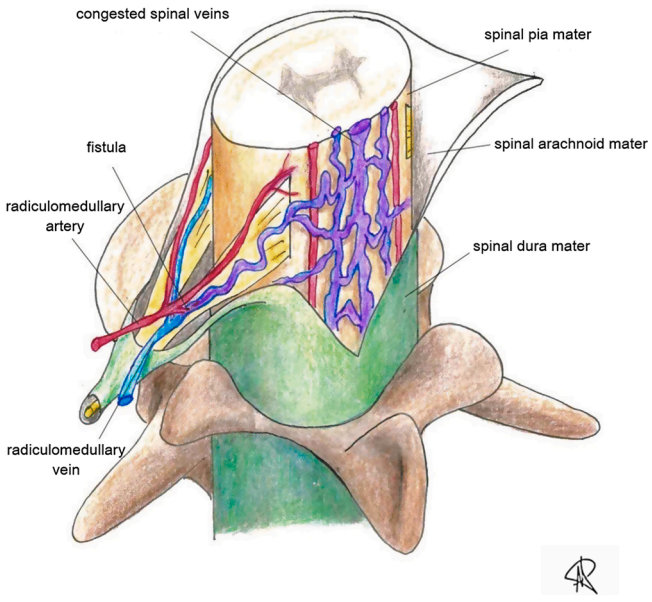

Fig. 6. Spinal dural arteriovenous fistula (SDAVF): a low-flow shunt between a radiculomeningeal artery and a medullary vein inside the dura mater results in vein arterialization and retrograde blood flow into a congested coronal venous plexus.

4.1. Arterial spinal cord ischemia (SCI)

Spinal cord arterial ischemia (SCI) is rare condition, accounting for less than 1% of all infarcts [45] and 5–8 % of acute myelopathies [46], with greater prevalence in the sixth-seventh decade of life [47].

SCI most commonly involves the territory of the ASA at the lower thoracic level [48].

The causes are heterogeneous and, in most cases, remain unclear.

The most common risk factor in adults is atheromatosis and the most common cause is thoraco-abdominal aortic surgery [7], because of atheroembolism, ligation or obstruction of the segmental branches of the aorta, or hypoperfusion. Vertebral or aortic dissections, prothrombotic states, drugs and especially fibrocartilaginous embolization following strenuous physical exercise or trauma often underlie SCI in younger patients; in the elderly arteriosclerosis, hypotension, acute heart failure are more common and should be considered [45].

SCI may also complicate spinal surgery, spinal angiography, and percutaneous spinal procedures [45]. However, 20 %–40 % of cases remain cryptogenic.

Onset of SCI is dramatic and hyperacute, with symptom nadir within 4 h, differently from other causes of myelopathy and similarly to spinal haemorrhage. Symptoms and MR patterns reflect the vascular territory involved. The anterior horns of grey matter and anterior tracts are affected, bilaterally or unilaterally, in case of ASA infarction [46] with subsequent damage of corticospinal, spinothalamic, and sympathetic tracts; the most common pattern is the non-specific "owl-eyes sign" on axial scan, due to anterior horns cells ischemia in case of incomplete syndrome of ASA and observed also in cervical stenosis-related myelopathy; in the sagittal plan it corresponds to a *pencil-like* appearance. The posterior columns and/or the surrounding white matter are affected in case of posterior spinal artery infarct. The damage may involve grey matter alone, due to the lower resistance of motoneurons to anoxia, or white and grey matter together [45]. Less typical clinical presentations include sulcocommissural syndrome, infarction at the conus medullaris level, central spinal infarcts and transverse medullary infarction.

MR in hyperacute and acute phases shows reduction of the apparent diffusion coefficient (ADC) and increase of the T2 signal intensity with

Fig. 7. Contrast enhanced CT in in a 65-year-old man with accidental fall and progressive lower limb weakness. Sagittal (a, b) and coronal (c) images demonstrate the early appearance of a serpiginous vascular structure along the posterior profile of the spinal cord between D10 and D11. Axial scan (d) confirms the posterior perimedullary anomalous vascular structure characterized by early enhancement after administration of contrast medium (white arrows in a, b, c and d).

slight spinal cord swelling affecting a long segment; the diffusion restriction, consistent with cytotoxic oedema, has the highest sensitivity for detecting spinal cord ischemia and it remains for the first week [49] (Fig. 5). In the acute phase there is no enhancement, that appears later on, and it helps in the differential. In the chronic phase atrophy may be observed. Considering the shared vascularization of the vertebral body, the disc and the spinal cord, high T2 signal of the bone and the disc, expression of infarction, may be seen at the same level [50].

Therapeutic interventions for SCI are intended to improve spinal cord perfusion by the modulation of both blood and CSF pressure, even though spinal fluid drainage. Thrombolysis is not indicated; corticosteroids instead are useful for patients with vasculitis [7].

4.2. Venous spinal cord ischemia

4.2.1. Spinal dural arteriovenous fistulas (SDAVFs)

Spinal cord congestion due to impaired venous drainage is a well-known cause of chronic myelopathy, potentially leading to venous ischemia. Spinal SDAVFs are the most common spinal vascular malformations, of unknown etiology, accounting for 70–85 % of spinal shunts

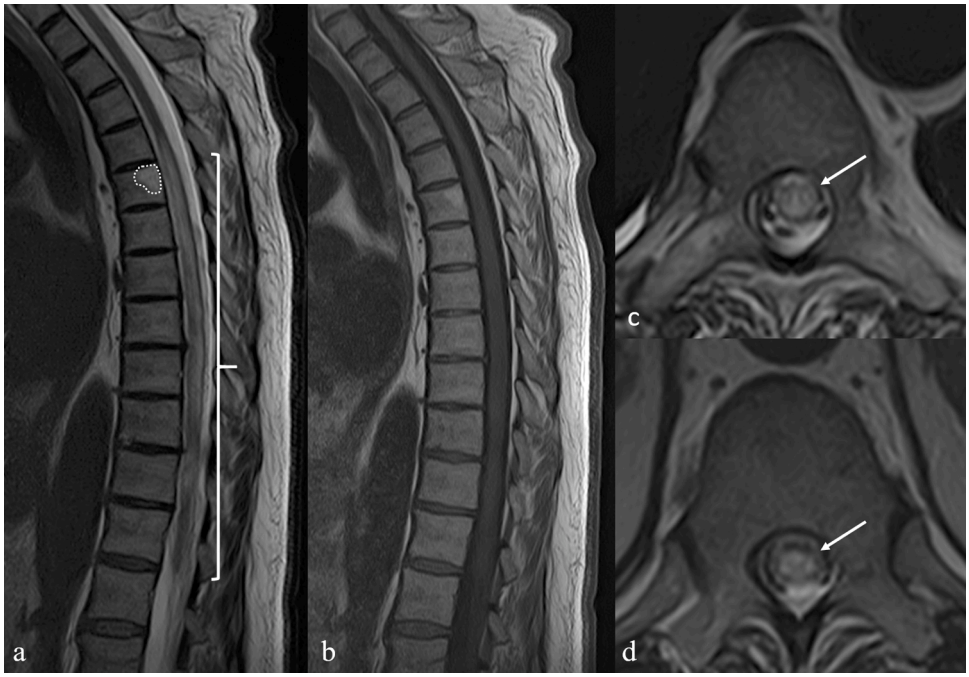

Fig. 8. MRI of the same patient in Fig. 7. Sagittal T2-TSE weighted (a) and T1-TSE weighted (b) images; axial T2-TSE weighted images at D7 (c) and D11 (d). T2 sequences show abnormal hyperintensity and swollen appearance of the dorsal spinal cord with cross-sectional involvement (bracket in a, white arrows in c and d). Vertebral haemangioma in D5 (white dotted line in a).

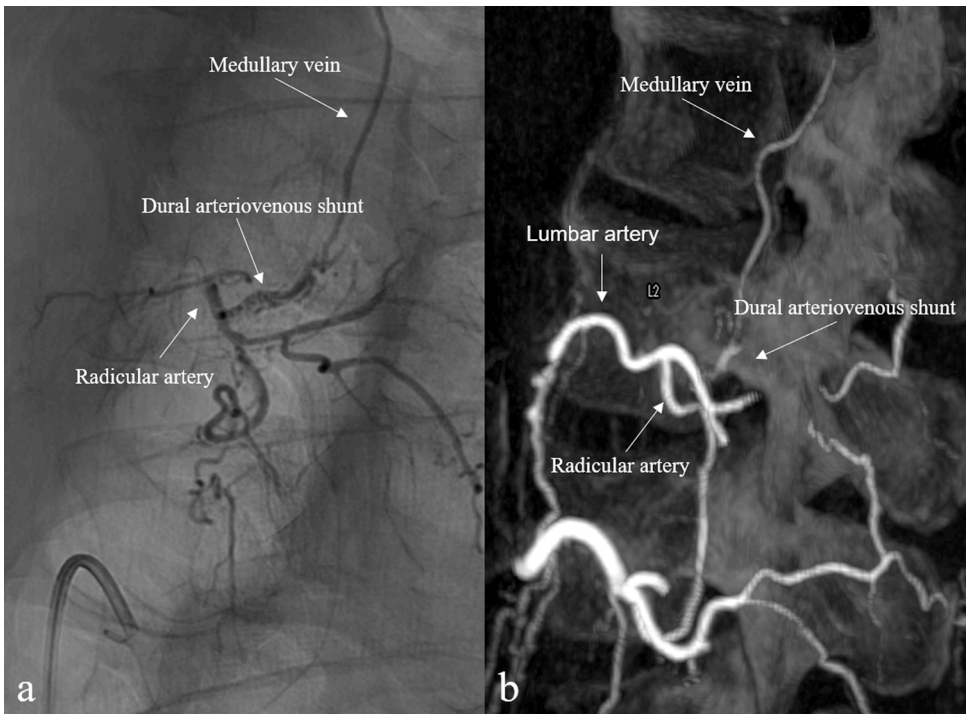

Fig. 9. Spinal dural arteriovenous fistula (SDAVF). Microcatheterism (A) and 3D reconstruction (B) following injection of the right L3 segmental artery show an anomalous arteriovenous shunt between a radiculomeningeal artery and a medullary vein, located underneath the vertebral pedicle.

[51] with annual incidence of 5–10 cases/1.000.000 [52]. Thoracolumbar region is the most commonly affected.

SDAVFs are anomalous shunts between a radiculomedullary artery and a medullary vein [53], classically located underneath the vertebral pedicle, inside the dura mater [54] (Figs. 6 and 7). Vein arterialization results in impaired drainage of normal spinal veins and venous congestion, with consequent intramedullary oedema, decreased arterial perfusion and chronic hypoxia [54]. Over time, venous congestion due to SDAVFs may affect additional spinal levels in an ascending fashion [49]. Sensorimotor disturbances are the most common symptoms and usually worsen with manoeuvres that exacerbate the venous congestion, such as exercise, prolonged standing, and the Valsalva manoeuvre. Sensory symptoms (numbness or hypoesthesia) may localize into the perianal area, while a sensory level occurs up to one-third of patients. Legs weakness includes upper and lower motor neuron features. Dysautonomia (bowel, bladder, and sexual dysfunction) is more tardive [7].

Detection of SDAVFs is tricky, due to nonspecific symptoms; diagnostic delays are common and significantly influence prognosis and good patients' outcome.

Classical MR imaging findings include, on T2 WI, centro-medullary spinal cord hyperintensity, as a result of intramedullary oedema affecting a long segment (LETM), and multiple flow voids from dilated veins on the cord surface [55], better recognized on heavily T2-weighted sequences as fast imaging employing steady-state acquisition (FIESTA) or 3D-TSE. Contrast administration may be useful in enhancing dilated and tortuous perimedullary veins, detecting small shunt [54], showing cord enhancement as consequence of the breakdown of the blood-spinal cord barrier due to venous hypertension (Fig. 8). Zalewski et al. showed a unique enhancement pattern in 43 % of patients with enhancing SDAVF, the larger majority in their study, called "the missing piece sign" and defined as at least one focal geographic non-enhancing area within a long segment of intense holocord gadolinium enhancement; in the segments without enhancement the blood-brain barrier is not disrupted thanks to a better venous drainage [56]. After treatment, edema disappears with *restitutio ad integrum* or SC gliosis-atrophy.

DSA is mandatory if a SDAVFs is suspected: a "*T-shaped*" anastomosis

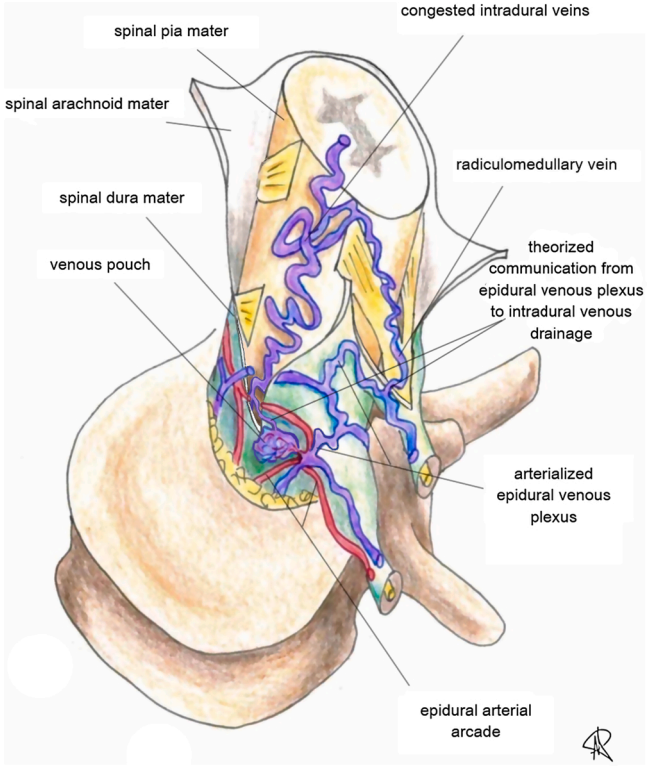

Fig. 10. Spinal epidural arterovenous fistula (SEDAVF) with peri-medullary drainage: the arteriovenous shunt is located in the epidural space and consists of a large dilated extradural venous pouch; spinal and paraspinal veins arise from the pouch, leading to spinal cord congestion.

Fig. 11. MRI in a 58-year-old man suffering from myelopathic symptoms in the past 18 months. Sagittal T2-weighted (a), T1-weighted (b) and contrast-enhanced T1-weighted (c) MRI images demonstrate enlargement and inhomogeneous T2 hyperintensity of the spinal cord between D8 and L1 (white bracket in a) with vanished enhancement after administration of gadolinium-based contrast medium (white bracket in c). Axial T2-weighted image (d) at level of D10 confirms the cross-sectional involvement of the spinal cord (white arrow).

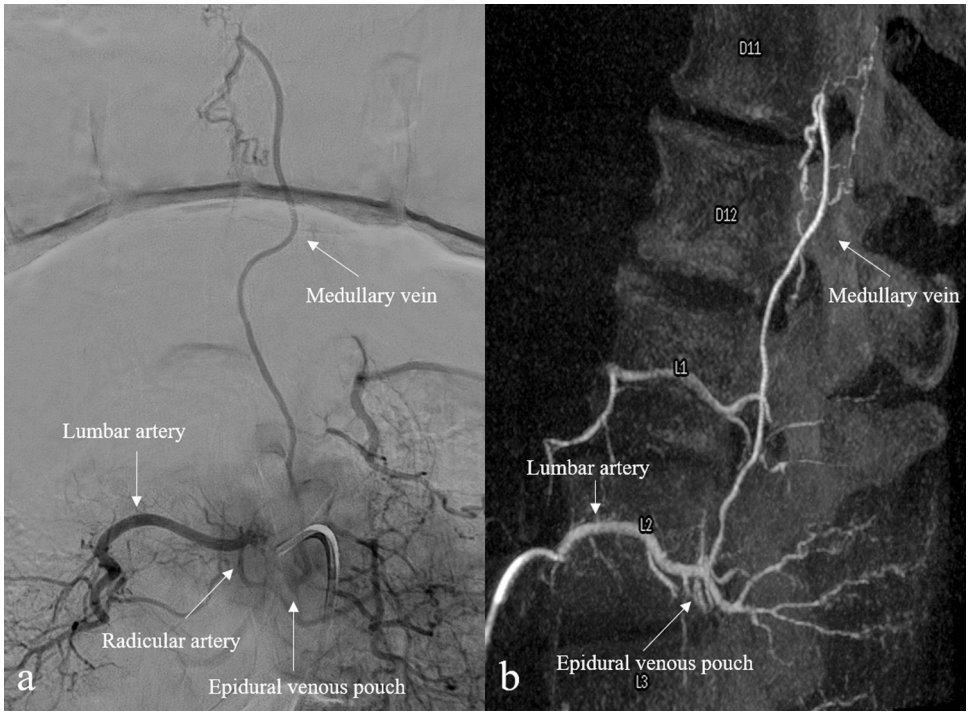

Fig. 12. Spinal epidural arteriovenous fistula (SEDAVF) with intradural venous drainage of the same patient in Fig. 11. Digital subtraction angiography (A) and 3D reconstruction (B) following injection of the right L2 segmental artery demonstrate a venous pouch in the epidural space and an intradural draining vein.

between the injected RMA and the draining vein is shown [57], as well as a network of dilated perimedullary veins [54] (Fig. 9).

Therapeutic options include either surgical and endovascular approaches aimed to disconnect the draining vein from its arterial supply [7].

4.2.2. *Cognard type V intracranial DAVFs*

Based on the same pathophysiology of SDAVFs, the Cognard type V intracranial DAVFs often present with progressive congestive myelopathy following venous drainage into peri-medullary veins [51].

4.2.3. *Spinal epi-dural arteriovenous fistulas (SEDAVFs)*

Spinal epidural arteriovenous fistulas (SEDAVFs) with peri-medullary drainage may themselves lead to spinal cord venous congestion [58]. These vascular malformations are usually clinically indistinguishable from SDAVFs, but symptoms result from venous hypertension and vasogenic oedema as a consequence of an arteriovenous shunt located in the epidural space and draining into intradural veins [59] (Fig. 10). MR imaging features of SEDAVFs with peri-medullary drainage are usually comparable to those typical of SDAVFs and the angioarchitecture of the lesion, including arterial feeders and venous drainage, is usually assessed with DSA (Fig. 11).

Some angiographic clues are helpful in distinguish SEDAVFs from SDAVFs, even if their discrimination may be challenging. A dilated extradural venous pouch is commonly detected in SEDAVFs, leading to spinal and paraspinal veins opacification; moreover, as most SEDAVFs are located in lumbosacral spine, the site of shunt is usually anterior, given the large ventral epidural space at this level (Figs. 12 and 13).

4.3. *Non-traumatic hematomyelia*

Main causes of non-traumatic hematomyelia (hemorrhage within the spinal cord in the absence of trauma) are the spinal arteriovenous malformations (AVMs) and the spinal cavernomas (SCs) [60].

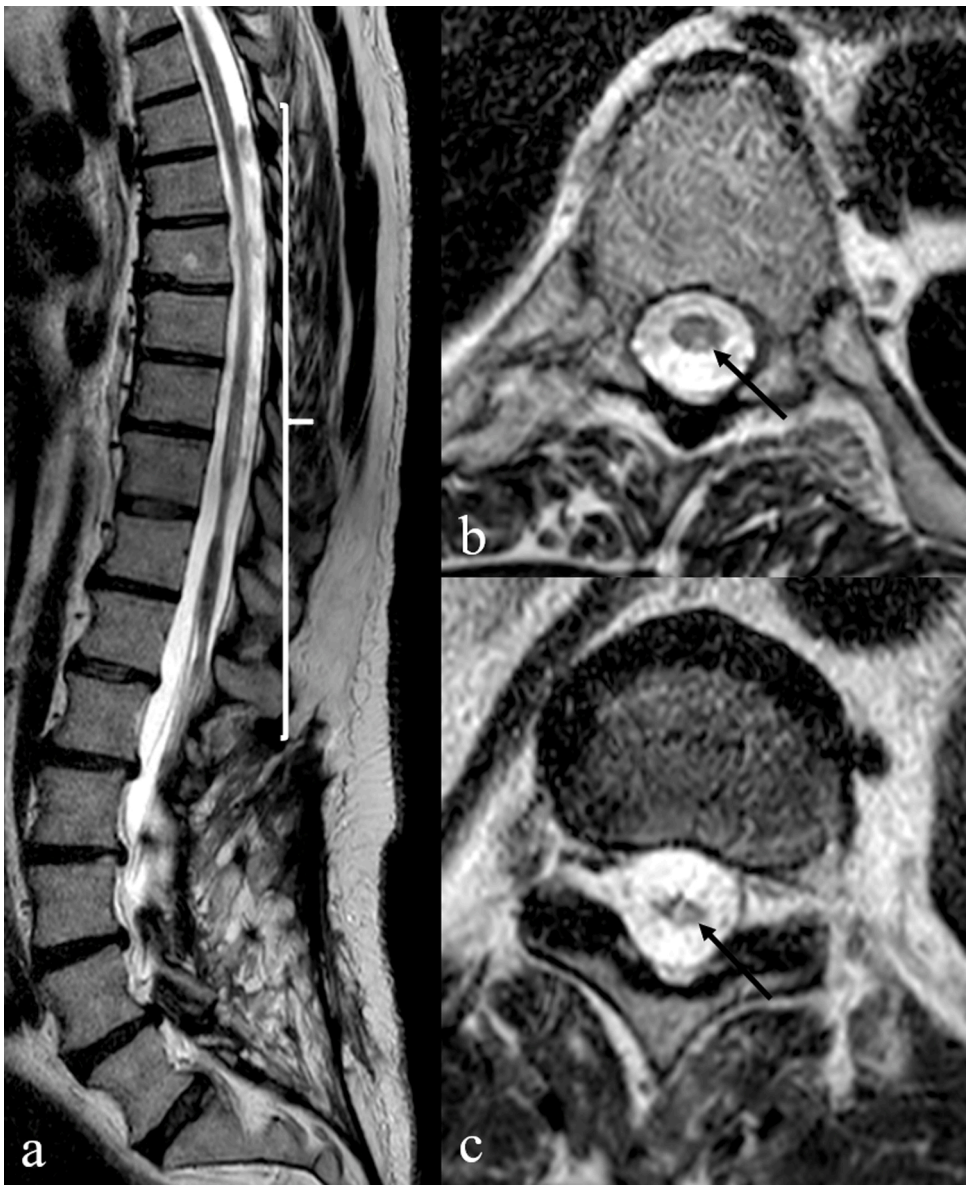

Fig. 13. Follow-up MRI scan of the same patient in Figs. 11 and 12. Sagittal (a) and axial (b, c) T2-weighted images show the severe reduction of dorsal spinal cord thickness (white bracket in a). Axial images demonstrate mild hyperintensity in the posterior median column at D8 (black arrow in b); to note the severe thinning and T2 hyperintensity of the spinal cord at D10-D11 (black arrow in c).

4.3.1. Spinal arteriovenous malformations (SAVMs)

Spinal arteriovenous malformations (SAVMs) are rare congenital high-flow vascular lesions [61], accounting for about 10–15 % of all spinal vascular shunts [7]; SAVMs may occur as sporadic or in the setting of genetic syndromes [62]. Intramedullary glomus-type AVMs (type II sec. Takay [63]) consist of an intramedullary *nidus* of shunting vessels usually located in the anterior half of the spinal cord [64] fed by one or more spinal arteries, draining into spinal veins (Fig. 14). Most of SAVMs are confined in the thoracic spine [65]; intranidal or arterial aneurysms are common, found in up to 30–40 % of SAVMs [7], and responsible of subarachnoid haemorrhage or hematomyelia, experienced in over half of patients with SAVMs [61].

Hematomyelia occurs in approximately one-half of patients and manifests with severe back, neck, or radicular pain along with sensorimotor/autonomic deficits corresponding to the spinal level involved (mostly thoracic). In non-hemorrhagic spinal AVMs, gradual myelopathic symptoms occur as result of mass effect, vascular steal, venous thrombosis, or venous congestion [7].

Conventional angiography is the gold standard for diagnosis and assessment of SAVMs. DSA allows recognition of feeding arteries and draining veins, provides information on the extension of the *nidus* and his relationship with feeding vessels, as well as enables the identification of fragility points as arterial aneurysms, pseudoaneurysms or fistula points.

Endovascular embolization and surgery are the therapeutic choices for spinal AVMs, although the eradication could be often incomplete and the risk for spinal cord ischemia increased. Stereotactic radiosurgery can be curative in some cases or facilitates the lesion's shrinking [7].

4.3.2. Spinal cavernomas

Spinal cavernomas (SC) or cavernous angiomas are rare slow-flow non-shunting vascular malformations, with no significant feeding artery or veins [7]; incidence rate of SC stands at 0.4−0.5% in the general population [66]. They are composed of a rich network of sinusoids and cavernous spaces, surrounded by gliosis and hemosiderin-containing macrophages [49] and are most often intramedullary, usually located

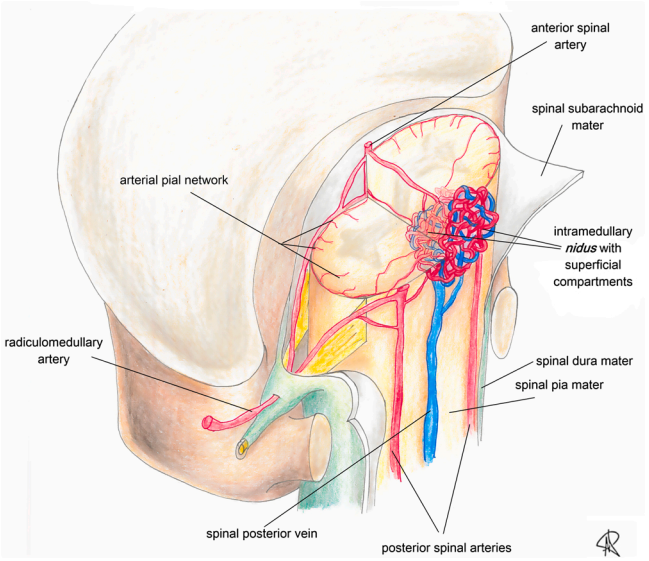

Fig. 14. Intramedullary glomus-type arteriovenous malformations (AVMs): a compact intramedullary nidus, with or without superficial nidus compartments, supplied by multiple feeding vessels from spinal arteries and draining into spinal veins.

at cervical or thoracic level. Clinically, SC may be an incidental finding on spine MR or typically produce episodic sensorimotor symptoms below the lesion level, although acute neurological deterioration may be consequence of sudden intralesional bleeding [61].

MR is the gold standard imaging modality to detect spinal cavernomas. They usually have heterogeneous MR signal on T1- and T2-WI, due to blood products in various stages of breakdown as consequence of thrombosis and haemorrhage, showing a typical "*popcorn-like*" mixed signal. Intralesional hyperintensity on T1-WI depicts recent bleeding, due to the presence of methaemoglobin; a well-circumscribed hypointense rim is usually noticed on T2-WI, representing hemosiderin deposited around cavernomas after clearance from the central area [67]. However, the T1 and T2 signals heterogeneity may be not shown in small SC which typically have focal low signal on T2-WI (Fig. 15).

Referring to the classification of SC for clinicians and neurosurgeons is quite important to define the type of SC: to this aim SC are divided in four different type:

-Type 1: Subacute haemorrhage. SC shows high signal intensity core on T1-WI and high or low signal intensity cores on T2-WI;

-Type 2: Mixed subacute and chronic (popcorn lesion). SC shows reticulated and mixed-signal intensity on both T1- and T2-WI with dark rim in T2-WI;

-Type 3: Chronic. SC shows iso or low signal intensity on T1-WI and low signal intensity with surrounding dark rim on T2-WI;

-Type 4: Small punctate hypointensity on T2-GRE images.

The use of gradient-echo or SWI sequences will show a "blooming" artefact from the presence of blood products; after contrast administration, enhancement is usually absent or minimal [49]. Cord oedema surrounding cavernomas is generally absent, as well as mass effect, except in case of intralesional bleeding [67]. Conventional angiography is unremarkable, as cavernomas lack direct arterial feeding and it is termed as angiographically occult vascular malformation [68].

Although dark rim on T2-WI is strongly suggestive, it is not indicative of SC as it might be shown in 22–33 % of spinal cord ependymomas in which is commonly termed "cap sign" along the border [69].

Thereby the differentiation between SC and haemorrhagic ependymomas is a critical issue. Jeon et al. suggested that eccentric axial location, the small size, the minimal enhancement without perilesional edema are more frequently observed in cavernous angioma than haemorrhagic ependymoma [70]. SC frequently involved one vertebral segment while spinal ependymoma might involve more vertebral segments; moreover, spinal ependymomas have an intrinsic slow growth rate contrary to SC which growth seems to be related to extrinsic factors as haemorrhage or growth of the cavernous matrix [71].

The presence of haemorrhage in SC has been proposed as the mechanism underlying acute neurological symptoms and it is related to increasing of dimensions of SC.

Due to the poor growth rate, SC are treated with conservative management applied in asymptomatic, mildly symptomatic or older patients, leaving surgery only for selected and deserved cases [7].

4.3.3. Hematomyelia in radiation therapy

Radiation therapy (RT) induce segmental spinal cord changes included in the RT fields. The safety upper limit is of 55−60 Gy for a

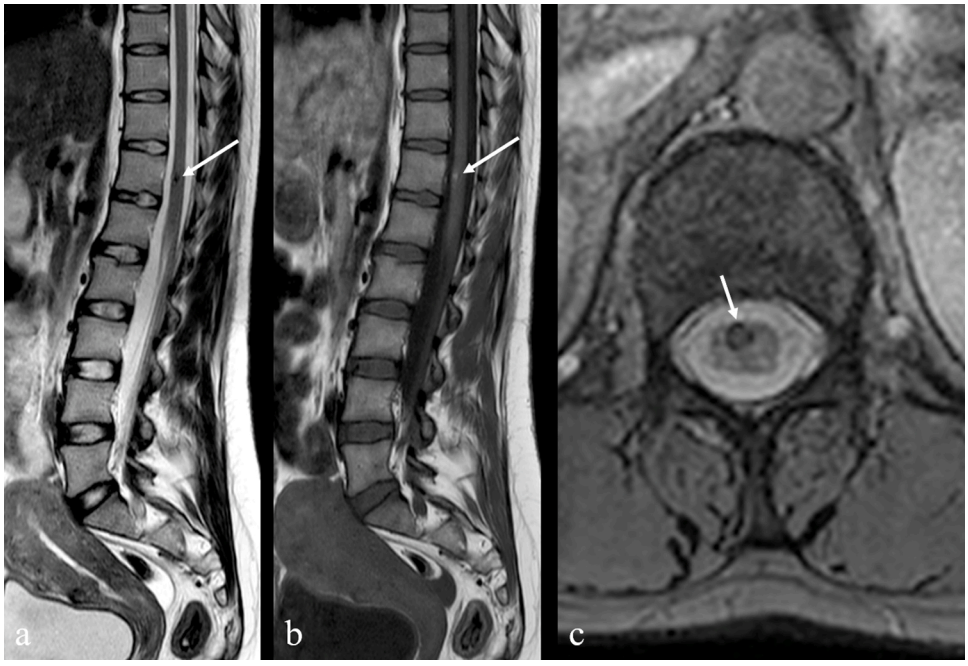

Fig. 15. Spinal cavernoma in a 22-year-old female patient with cerebral cavernomatosis. Sagittal T2-weighted (a) and T1-weighted (b) MR images demonstrate a nodular area of T2-hypointensity and T1-hyperintensity in the ventral spinal column at level D12 with slight and focal enlargement of the spinal cord (white arrows in a and b). Axial T2-GRE weighted MR image (c) confirms the intramedullary lesion with low signal intensity and blooming artifact related to the presence of blood products (white arrow in c). These findings are suggestive of spinal cavernoma.

restricted field with 1.8–2.0 Gy daily fractions; however, the specific patient sensitivity to RT is an unpredictable condition [72]. Even though radiation myelitis may be seen, the radiation-induced hematomyelia is an extremely rare condition and it seems to be related to a multifactorial alterations of the spinal cells and microenvironment [73]. Acute hematomyelia in RT is characterized by swelling of the spinal cord with T1-hyperintensity and T2 hypointense intremedullary lesion on MRI also with blood-fluid level; over the time hematomyelia showed T1 and T2 signal changes. After administration of contrast-medium no enhancement is detected.

Spinal angiography could be useful if MR shows abnormal vessel or enlarged vessels.

4.3.4. Intrasyringal haemorrhage

The first haemorrhage in a preexisting syringomyelic cavity was described by Gowers in 1904 [74]. It is a quite rare condition and until today have been reported fewer than 20 cases frequently associated with scoliosis or Chiari malformation Type I [75]. The intrasyringal haemorrhage is thought to be related to sudden dilatation of hydro-syringomyelic cavity with elongation and rupture of the intrasyringal vessels or from a torn intraspinal vein deprived of its normal glio-neural support [76,77]. MR is the gold standard to evaluate haemorrhage in hydro-syringomyelic cavity: usually it shown a fluid-fluid level. However, the appearance of hemorrhage varies according to the phase of bleeding.

4.4. Spinal arteriovenous metameric syndrome (Cobb syndrome)

Cobb syndrome is a rare, non-inherited congenital disorder characterized by the involvement of all vessels within an embryonic metamere [47], leading to the presence of spinal vascular malformations associated with cutaneous vascular lesion involving the same metamere. To date, prevalence is unknown and approximately 100 cases have been reported in literature [78].

Dermatological manifestations mainly include *nevus flammeus* and angiokeratomas; spinal vascular lesions consist of high-flow arteriovenous shunts like SDAVFs and AVMs, whose extension may involve meninges, vertebral bodies and soft tissue within the same metamere [79], as well as low-flow non-arterialized vascular malformations [80]. Symptoms may result from spinal cord compression, ischemia, venous hypertension or subarachnoid haemorrhage [81]; in case of vascular cutaneous malformation with metameric distribution, Cobb syndrome should be considered.

5. Conclusion

Vascular myelopathies are critical conditions with acute/subacute presentation and severe consequences on the quality of life. The pathogenic mechanism in vascular myelopathies may be either an impaired arterial blood supply or venous drainage, with different underlying causes.

Radiological imaging, correctly addressed by the clinical onset and metameric level of symptoms, is essential for the correct diagnosis and includes both MR and CT angiography. Once the cause is suspected or identified, DSA is crucial for the detailed evaluation of spinal cord vascular anatomy in order to plan the treatment.

Ethical statement

All procedures performed in studies involving human participants were in accordance with the ethical standards of the institutional and/or national research committee and with the 1964 Helsinki declaration and its later amendments or comparable ethical standards.

Funding

This research did not receive any specific grant from funding agencies in the public, commercial, or not-for-profit sectors.

Declaration of Competing Interest

The authors declare that they have no conflict of interest.

Acknowledgement

Thanks to Dr. Noemi Pucci for drawing the illustrations.

References

[1] A. Santillan, V. Nacarino, E. Greenberg, et al., Vascular anatomy of the spinal cord, J. Neurointerv. Surg. 4 (4) (2012) 67–74, https://doi.org/10.1136/neurintsurg-2011-010018.
[2] T. Becske, P.K. Nelson, The vascular anatomy of the vertebro-spinal Axis, Neurosurg. Clin. N. Am. 20 (3) (2009) 259–264, https://doi.org/10.1016/j.nec.2009.03.002.
[3] A.N. Bosmia, E. Hogan, M. Loukas, et al., Blood supply to the human spinal cord: part I. Anatomy and hemodynamics, Clin. Anat. 28 (1) (2015) 52–64, https://doi.org/10.1002/ca.22281.
[4] P. Gailloud, Introduction to diagnostic and therapeutic spinal angiography, Neuroimaging Clin. N. Am. 29 (4) (2019) 595–614, https://doi.org/10.1016/j.nic.2019.07.008.
[5] M.K.Y. Hong, M.K.H. Hong, W.R. Pan, et al., The angiosome territories of the spinal cord: exploring the issue of preoperative spinal angiography: laboratory investigation, J. Neurosurg. Spine 8 (4) (2008) 352–364, https://doi.org/10.3171/SPI/2008/8/4/352.
[6] D. Taterra, B. Skinningsrud, P.A. Pękala, et al., Artery of Adamkiewicz: a meta-analysis of anatomical characteristics, Neuroradiology 61 (8) (2019) 869–880, https://doi.org/10.1007/s00234-019-02207-y.
[7] C.L. Kramer, Vascular disorders of the spinal cord, Contin. Lifelong Learn. Neurol. 24 (2) (2018) 407–426, https://doi.org/10.1212/CON.0000000000000595.
[8] N. Nathoo, E.C. Caris, J.A. Wiener, E. Mendel, History of the vertebral venous plexus and the significant contributions of breschet and batson, Neurosurgery 69 (5) (2011) 1007–1014, https://doi.org/10.1227/NEU.0b013e3182274865.
[9] L.M. Shah, C.J. Hanrahan, MRI of spinal bone marrow: part 1, techniques and normal age-related appearances, Am. J. Roentgenol. 197 (6) (2011) 1298–1308, https://doi.org/10.2214/AJR.11.7005.
[10] K. Hittmair, R. Mallek, D. Prayer, et al., Spinal cord lesions in patients with multiple sclerosis: comparison of MR pulse sequences, Am. J. Neuroradiol. 17 (8) (1996) 1555–1565.
[11] M. Mascalchi, G. Dal Pozzo, C. Bartolozzi, Effectiveness of the Short TI Inversion Recovery (STIR) sequence in MR imaging of intramedullary spinal lesions, Magn. Reson. Imaging 11 (1) (1993) 17–25, https://doi.org/10.1016/0730-725X(93)90407-5.
[12] J.W. Thorpe, D.G. MacManus, B.E. Kendall, et al., Short tau inversion recovery fast spin-echo (fast STIR) imaging of the spinal cord in multiple sclerosis, Magn. Reson. Imaging 12 (7) (1994) 983–989, https://doi.org/10.1016/0730-725X(94)91228-O.
[13] J.C.J. Bot, F. Barkhof, À Lycklama, G.J. Nijeholt, et al., Comparison of a conventional cardiac-triggered dual spin-echo and a fast STIR sequence in detection of spinal cord lesion in multiples sclerosis, Eur. Radiol. 10 (5) (2000) 753–758, https://doi.org/10.1007/s003300050998.
[14] J.L. Dietemann, A. Bogorin, M. Abu Eid, et al., Tips and traps in neurological imaging: imaging the perimedullary spaces, Diagn. Interv. Imaging 93 (12) (2012) 985–992, https://doi.org/10.1016/j.diii.2012.08.005.
[15] N. Martin, D. Malfair, Y. Zhao, et al., Comparison of MERGE and axial T2-weighted fast spin-echo sequences for detection of multiple sclerosis lesions in the cervical spinal cord, Am. J. Roentgenol. 199 (1) (2012) 157–162, https://doi.org/10.2214/AJR.11.7039.
[16] Y. Kumar, D. Hayashi, Role of magnetic resonance imaging in acute spinal trauma: a pictorial review, BMC Musculoskelet. Disord. 17 (2016), https://doi.org/10.1186/s12891-016-1169-6.
[17] M.I. Vargas, J.L. Dietemann, 3D T2-SPACE versus T2-FSE or T2 gradient recalled-echo: which is the best sequence? Am. J. Neuroradiol. 38 (7) (2017) E48–E49, https://doi.org/10.3174/ajnr.A5190.
[18] M.I. Vargas, J. Boto, T.R. Meling, Imaging of the spine and spinal cord: an overview of magnetic resonance imaging (MRI) techniques, Rev. Neurol. (Paris) 177 (5) (2021) 451–458, https://doi.org/10.1016/j.neurol.2020.07.005.
[19] M.I. Vargas, B.M.A. Delattre, J. Boto, et al., Advanced magnetic resonance imaging (MRI) techniques of the spine and spinal cord in children and adults, Insights Imaging 9 (4) (2018) 549–557, https://doi.org/10.1007/s13244-018-0626-1.
[20] M.I. Vargas, J. Gariani, R. Sztajzel, et al., Spinal cord ischemia: practical imaging tips, pearls, and pitfalls, AJNR. Am. J. Neuroradiol. 36 (5) (2015) 825–830, https://doi.org/10.3174/ajnr.A4118.
[21] M.I. Vargas, J. Delavelle, H. Jlassi, et al., Clinical applications of diffusion tensor tractography of the spinal cord, Neuroradiology 50 (1) (2008) 25–29, https://doi.org/10.1007/s00234-007-0309-y.

[22] F. Di Giuliano, E. Picchi, M. Muto, et al., Radiological imaging in multiple myeloma: review of the state-of-the-art, Neuroradiology 62 (8) (2020) 905–923, https://doi.org/10.1007/s00234-020-02417-9.
[23] S. Mirafzal, A. Goujon, R. Deschamps, et al., 3D PSIR MRI at 3 Tesla improves detection of spinal cord lesions in multiple sclerosis, J. Neurol. 267 (2) (2020) 406–414, https://doi.org/10.1007/s00415-019-09591-8.
[24] F. Di Giuliano, S. Minosse, E. Picchi, et al., Comparison between synthetic and conventional magnetic resonance imaging in patients with multiple sclerosis and controls, Magn Reson Mater Physics, Biol Med. 33 (4) (2019) 549–557, https://doi.org/10.1007/s10334-019-00804-9.
[25] M.I. Vargas, M. Drake-Pérez, B.M.A. Delattre, et al., Feasibility of a synthetic MR imaging sequence for spine imaging, Am J Neuroradiol. 39 (9) (2018) 1756–1763, https://doi.org/10.3174/ajnr.A5728.
[26] G. Zhou, M.H. Li, C. Lu, et al., Dynamic contrast-enhanced magnetic resonance angiography for the localization of spinal dural arteriovenous fistulas at 3T, J. Neuroradiol. 44 (1) (2017) 17–23, https://doi.org/10.1016/j.neurad.2016.10.002.
[27] Y.W. Nielsen, H.S. Thomsen, Contrast-enhanced peripheral MRA: technique and contrast agents, Acta radiol. 53 (7) (2012) 769–777, https://doi.org/10.1258/ar.2012.120008.
[28] A. Lindenholz, K.G. TerBrugge, J.M.C. van Dijk, R.I. Farb, The accuracy and utility of contrast-enhanced MR angiography for localization of spinal dural arteriovenous fistulas: the Toronto experience, Eur. Radiol. 24 (11) (2014) 2885–2894, https://doi.org/10.1007/s00330-014-3307-6.
[29] H. Parmar, M.K. Ivancevic, N. Dudek, et al., Neuroradiologic applications of dynamic MR angiography at 3 t, Magn. Reson. Imaging Clin. N. Am. 17 (1) (2009) 63–75, https://doi.org/10.1016/j.mric.2009.01.004.
[30] M.I. Vargas, I. Barnaure, J. Gariani, et al., Vascular imaging techniques of the spinal cord, Semin Ultrasound, CT MRI 38 (2) (2017) 143–152, https://doi.org/10.1053/j.sult.2016.07.004.
[31] J.B. Cao, L.L. Cui, X.Y. Jiang, et al., Clinical application and diagnostic value of noninvasive spinal angiography in spinal vascular malformations, J. Comput. Assist. Tomogr. 38 (3) (2014) 474–479, https://doi.org/10.1097/RCT.0b013e3182ab3ab6.
[32] K.D. Than, J.R. Sangala, A.C. Wang, et al., The current status and recent advances in high-resolution imaging of spinal vascular malformations, J. Clin. Neurosci. 20 (1) (2013) 66–71, https://doi.org/10.1016/j.jocn.2012.05.008.
[33] E. Orru, C.O.A. Tsang, J.M. Klostranec, V.M. Pereira, Republished: transradial approach in the treatment of a sacral dural arteriovenous fistula: a technical note, J. Neurointerv. Surg. 11 (8) (2019) e4, https://doi.org/10.1136/neurintsurg-2019-014834.rep.
[34] A.L. Kühn, K. De Macedo Rodrigues, J. Singh, et al., Distal radial access in the anatomical snuffbox for neurointerventions: a feasibility, safety, and proof-of-concept study, J. Neurointerv. Surg. 12 (8) (2020) 798–801, https://doi.org/10.1136/neurintsurg-2019-015604.
[35] J. Haynes, E. Nossek, M. Shapiro, et al., Radial arterial access for thoracic intraoperative spinal angiography in the prone position, World Neurosurg. 137 (2020) e358–e365, https://doi.org/10.1016/j.wneu.2020.01.208.
[36] K.W. Joung, K.H. Yang, W.J. Shin, et al., Anesthetic consideration for neurointerventional procedures, Neurointervention 9 (2) (2014) 72–77, https://doi.org/10.5469/neuroint.2014.9.2.72.
[37] J.D. Rabinov, T.M. Leslie-Mazwi, J.A. Hirsch, Diagnostic angiography of the cerebrospinal vasculature. Handbook of Clinical Neurology, 2016, pp. 151–163, 135 Eselvier.
[38] P. Barreras, D. Heck, B. Greenberg, et al., Analysis of 30 spinal angiograms falsely reported as normal in 18 patients with subsequently documented spinal vascular malformations, Am. J. Neuroradiol. 38 (9) (2017) 1814–1819, https://doi.org/10.3174/ajnr.A5275.
[39] T.D. Aadland, K.R. Thielen, T.J. Kaufmann, et al., 3D C-arm conebeam CT angiography as an adjunct in the precise anatomic characterization of spinal dural arteriovenous fistulas, Am. J. Neuroradiol. 31 (3) (2010) 476–480, https://doi.org/10.3174/ajnr.A1840.
[40] Y. Ozpeynirci, B. Schmitz, M. Schick, R. Konig, Role of three-dimensional rotational angiography in the treatment of spinal dural arteriovenous fistulas, Cureus 9 (12) (2017) e1932, https://doi.org/10.7759/cureus.1932.
[41] R.F. Spetzler, P.W. Detwiler, H.A. Riina, R.W. Porter, Modified classification of spinal cord vascular lesions, J. Neurosurg. 96 (2) (2002) 145–156, https://doi.org/10.3171/spi.2002.96.2.0145.
[42] C. Islak, N. Kocer, Imaging of vascular disorders of the spine and spinal cord. Clinical Neuroradiology, Springer International Publishing, 2019, pp. 2067–2099.
[43] S. Marziali, E. Picchi, F. Di Giuliano, et al., Acute disseminated encephalomyelitis following Campylobacter jejuni gastroenteritis: case report and review of the literature, Neuroradiol. J. 30 (1) (2017) 65–70, https://doi.org/10.1177/1971400916680123.
[44] W.F. Schmalstieg, B.G. Weinshenker, Approach to acute or subacute myelopathy, Neurology 75 (18) (2010) S2–S8, https://doi.org/10.1212/WNL.0b013e3181fb3638.
[45] S. Weidauer, M. Wagner, M. Nichtweiß, Magnetic resonance imaging and clinical features in acute and subacute myelopathies, Clin. Neuroradiol. 27 (4) (2017) 417–433, https://doi.org/10.1007/s00062-017-0604-x.
[46] N. Sarbu, V. Lolli, J.G. Smirniotopoulos, Magnetic resonance imaging in myelopathy: a pictorial review, Clin. Imaging 57 (2019) 56–68, https://doi.org/10.1016/j.clinimag.2019.05.002.
[47] S.M. Vuong, W.J. Jeong, H. Morales, T.A. Abruzzo, Vascular diseases of the spinal cord: infarction, hemorrhage, and venous congestive myelopathy, Semin Ultrasound, CT MRI 37 (5) (2016) 466–481, https://doi.org/10.1053/j.sult.2016.05.008.
[48] I. Kister, E. Johnson, E. Raz, et al., Specific MRI findings help distinguish acute transverse myelitis of Neuromyelitis Optica from spinal cord infarction, Mult. Scler. Relat. Disord. 9 (2016) 62–67, https://doi.org/10.1016/j.msard.2016.04.005.
[49] P.G. Kranz, T.J. Amrhein, Imaging approach to myelopathy: acute, subacute, and chronic, Radiol. Clin. North Am. 57 (2) (2019) 257–279, https://doi.org/10.1016/j.rcl.2018.09.006.
[50] G. Amoiridis, I. Ameridou, M. Mavridis, Intervertebral disk and vertebral body infarction as a confirmatory sign of spinal cord ischemia, Neurology 63 (9) (2004) 1755, https://doi.org/10.1212/01.WNL.0000142973.33952.68.
[51] L. Hacein-Bey, A.A. Konstas, J. Pile-Spellman, Natural history, current concepts, classification, factors impacting endovascular therapy, and pathophysiology of cerebral and spinal dural arteriovenous fistulas, Clin. Neurol. Neurosurg. 121 (2014) 64–75, https://doi.org/10.1016/j.clineuro.2014.01.018.
[52] C. Koch, Spinal dural arteriovenous fistula, Curr. Opin. Neurol. 19 (1) (2006) 69–75, https://doi.org/10.1097/01.wco.0000200547.22292.11.
[53] S. Fox, L. Hnenny, U. Ahmed, et al., Spinal dural arteriovenous fistula: a case series and review of imaging findings, Spinal Cord Ser. Cases 3 (2017) 17024, https://doi.org/10.1038/scsandc.2017.24.
[54] T. Krings, S. Geibprasert, Spinal dural arteriovenous fistulas, Am. J. Neuroradiol. 30 (4) (2009) 639–648, https://doi.org/10.3174/ajnr.A1485.
[55] F. Sheerin, K. Collison, G. Quaghebeur, Magnetic resonance imaging of acute intramedullary myelopathy: radiological differential diagnosis for the on-call radiologist, Clin. Radiol. 64 (1) (2009) 84–94, https://doi.org/10.1016/j.crad.2008.07.004.
[56] N.L. Zalewski, A.A. Rabinstein, W. Brinjikji, et al., Unique gadolinium enhancement pattern in spinal dural arteriovenous fistulas, JAMA Neurol. 75 (12) (2018) 1542–1545, https://doi.org/10.1001/jamaneurol.2018.2605.
[57] H. Kiyosue, Y. Matsumaru, Y. Niimi, et al., Angiographic and clinical characteristics of thoracolumbar spinal epidural and dural arteriovenous fistulas, Stroke 48 (12) (2017) 3215–3222, https://doi.org/10.1161/STROKEAHA.117.019131.
[58] W. Brinjikji, R. Yin, D.M. Nasr, G. Lanzino, Spinal epidural arteriovenous fistulas, J. Neurointerv. Surg. 8 (12) (2016) 1305–1310, https://doi.org/10.1136/neurintsurg-2015-012181.
[59] L. Rangel-Castilla, P.J. Holman, C. Krishna, et al., Spinal extradural arteriovenous fistulas: a clinical and radiological description of different types and their novel treatment with Onyx: clinical article, J. Neurosurg. Spine 15 (5) (2011) 541–549, https://doi.org/10.3171/2011.6.SPINE10695.
[60] A. Shaban, T. Moritani, S. Al Kasab, et al., Spinal cord hemorrhage, J. Stroke Cerebrovasc. Dis. 27 (6) (2018) 1435–1446, https://doi.org/10.1016/j.jstrokecerebrovasdis.2018.02.014.
[61] D.D. Do-Dai, M.K. Brooks, A. Goldkamp, et al., Magnetic resonance imaging of intramedullary spinal cord lesions: a pictorial review, Curr. Probl. Diagn. Radiol. 39 (4) (2010) 160–185, https://doi.org/10.1067/j.cpradiol.2009.05.004.
[62] H. Shallwani, M.Z. Tahir, M.E. Bari, Tanveer-Ul-Haq, Concurrent intracranial and spinal arteriovenous malformations: report of two pediatric cases and literature review, Surg. Neurol. Int. 3 (2012) 51, https://doi.org/10.4103/2152-7806.96074.
[63] K. Takai, Spinal arteriovenous shunts: angioarchitecture and historical changes in classification, Neurol. Med. Chir. (Tokyo) 57 (7) (2017) 356–365, https://doi.org/10.2176/nmc.ra.2016-0316.
[64] R. Singh, B. Lucke-Wold, K. Gyure, S. Boo, A review of vascular abnormalities of the spine, Ann. Vasc. Med. Res. 3 (4) (2016) 1045.
[65] B.A. Gross, R. Du, Spinal glomus (type II) arteriovenous malformations: a pooled analysis of hemorrhage risk and results of intervention, Neurosurgery 72 (1) (2013) 25–32, https://doi.org/10.1227/NEU.0b013e318276b5d3.
[66] G.H. Choi, K.N. Kim, S. Lee, et al., The clinical features and surgical outcomes of patients with intramedullary spinal cord cavernous malformations, Acta Neurochir. (Wien) 153 (8) (2011) 1677–1684, https://doi.org/10.1007/s00701-011-1016-3.
[67] J.C. Vilanova, J. Barceló, J.G. Smirniotopoulos, et al., Hemangioma from head to toe: MR imaging with pathologic correlation, Radiographics 24 (2) (2004) 367–385, https://doi.org/10.1148/rg.242035079.
[68] I. Sun, M. Necmettin Pamir, Spinal cavernomas: outcome of surgically treated 10 patients, Front. Neurol. 8 (2017) 672, https://doi.org/10.3389/fneur.2017.00672.
[69] M.J. Fine, I.I. Kricheff, D. Freed, F.J. Epstein, Spinal cord ependymomas: MR imaging features, Radiology 197 (3) (1995) 655–658, https://doi.org/10.1148/radiology.197.3.7480734.
[70] I. Jeon, W.S. Jung, S.H. Suh, et al., MR imaging features that distinguish spinal cavernous angioma from hemorrhagic ependymoma and serial MRI changes in cavernous angioma, J. Neurooncol. 130 (1) (2016) 229–236, https://doi.org/10.1007/s11060-016-2239-1.
[71] J.P. Houtteville, Brain cavernoma: a dynamic lesion, Surg. Neurol. 48 (6) (1997) 610–614, https://doi.org/10.1016/S0090-3019(96)00551-4.
[72] A. Agarwal, S. Kanekar, K. Thamburaj, K. Vijay, Radiation-induced spinal cord hemorrhage (hematomyelia), Neurol. Int. 6 (4) (2014) 5553, https://doi.org/10.4081/ni.2014.5553.
[73] I.C. Gibbs, C. Patil, P.C. Gerszten, et al., Delayed radiation-induced myelopathy after spinal radiosurgery, Neurosurgery 64 (2) (2009) A67–A72, https://doi.org/10.1227/01.NEU.0000341628.98141.B6.
[74] A Lecture ON SYRINGAL HÆMORRHAGE INTO THE SPINAL CORD. Lancet.
[75] A. Hamlat, M. Adn, M. Ben Yahia, et al., Gowers intrasyringal hemorrhage. Case report and review of the literature, J. Neurosurg. Spine 3 (6) (2005) 477–481, https://doi.org/10.3171/spi.2005.3.6.0477.

[76] P. Perot, W. Feindel, D. Lloyd-Smith, Hematomyelia as a complication of syringomyelia: gowers' syringal hemorrhage. Case report, J. Neurosurg. 25 (4) (1966) 447–451, https://doi.org/10.3171/jns.1966.25.4.0447.
[77] C.B. Sedzimir, J.R. Roberts, J.V. Occleshaw, P.H. Buxton, Gowers' syringal haemorrhage, J Neurol Neurosurg Psychiatry. 37 (3) (1974) 312–315, https://doi.org/10.1136/jnnp.37.3.312.
[78] F.S. Barros, V.H.R. Marussi, L.L.F. Amaral, et al., The rare neurocutaneous disorders update on clinical, molecular, and neuroimaging features, Top. Magn. Reson. Imaging 27 (6) (2018) 433–462, https://doi.org/10.1097/RMR.0000000000000185.
[79] E. Dilmé-Carreras, M. Iglesias-Sancho, G. Márquez-Balbás, et al., Cobb syndrome: case report and review of the literature, Dermatology 221 (2) (2010) 110–112, https://doi.org/10.1159/000313510.
[80] P. Pal, S. Ray, S. Chakraborty, et al., Cobb syndrome: a rare cause of paraplegia, Ann. Neurosci. 22 (3) (2015) 191–193, https://doi.org/10.5214/ans.0972.7531.220312.
[81] M. Tubridy Clark, E.L. Brooks, W. Chong, et al., Cobb syndrome: a case report and systematic review of the literature, Pediatr. Neurol. 39 (6) (2008) 423–425, https://doi.org/10.1016/j.pediatrneurol.2008.08.001.